

# **Hybrid Multivalent Jack Bean $\alpha$ -Mannosidase Inhibitors: The First Example of Gold Nanoparticles Decorated with Deoxynojirimycin Inhitopes**

**Costanza Vanni 1, Anne Bodlenner 2,\*<sup>,</sup> Marco Marradi 1, Jérémie P. Schneider 2, Maria de los Angeles Ramirez 3, Sergio Moya 3, Andrea Goti 1,4, Francesca Cardona 1,4, Philippe Compain 2 and Camilla Matassini 1,4,\***

1 Dipartimento di Chimica "Ugo Schiff", Università di Firenze, Via della Lastruccia 3-13, 50019 Sesto Fiorentino, Italy; costanza.vanni@unifi.it (C.V.); marco.marradi@unifi.it (M.M.); andrea.goti@unifi.it (A.G.); francesca.cardona@unifi.it (F.C.)

2 Laboratoire d'Innovation Moléculaire et Applications (LIMA), University of Strasbourg, University of Haute-Alsace, CNRS (UMR 7042), Equipe de Synthèse Organique et Molécules Bioactives (SYBIO), ECPM, 25 Rue Becquerel, 67000 Strasbourg, France; jeremy.schneider@live.fr (J.P.S.); philippe.compain@unistra.fr (P.C.)

3 Soft Matter Nanotechnology Lab, CIC biomaGUNE, Basque Research and Technology Alliance (BRTA), Paseo Miramón 182, 20014 Donostia-San Sebastián, Gipuzkoa, Spain; aangie.ramirez@gmail.com (M.d.l.A.R.); smoya@cicbiomagune.es (S.M.)

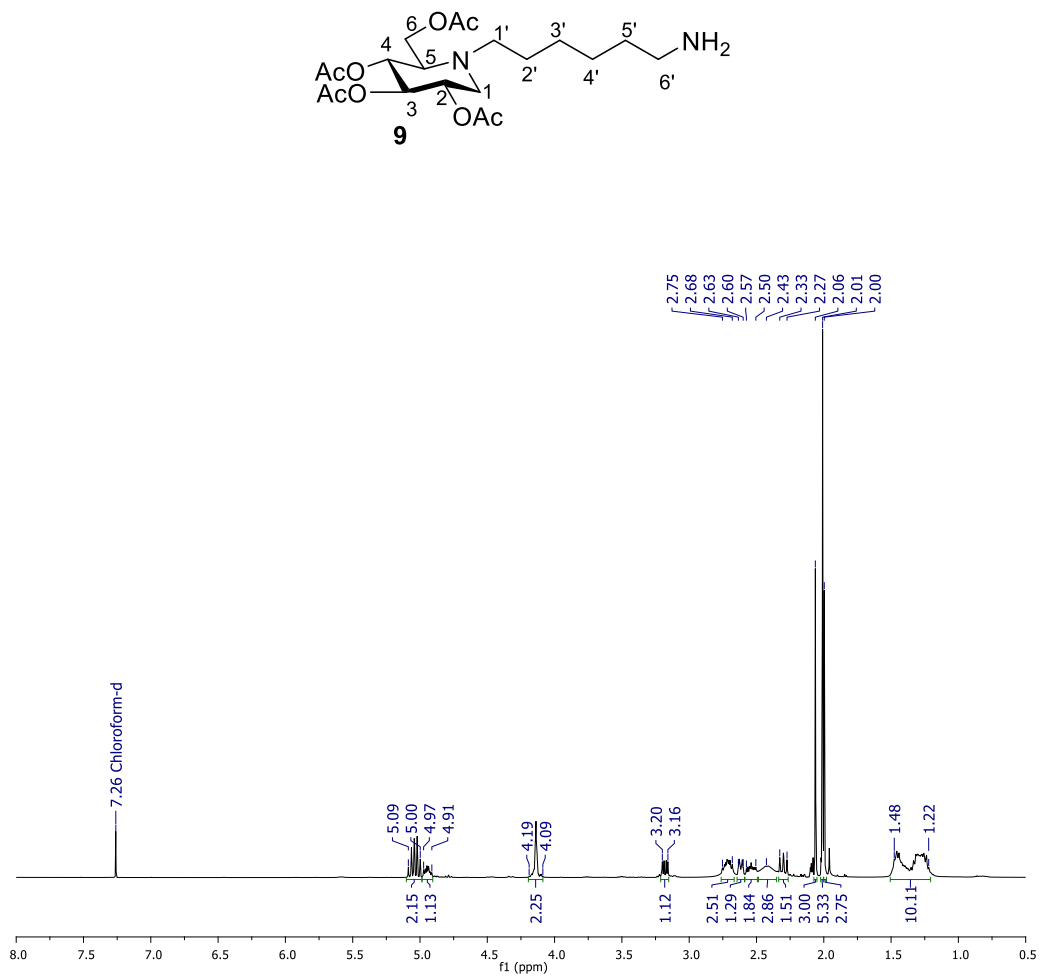
4 Associated with LENS, Via N. Carrara 1, 50019 Sesto Fiorentino, Italy

\* Correspondence: annebod@unistra.fr (A.B.); camilla.matassini@unifi.it (C.M.); Tel.: +33-36-8852684 (A.B.); +39-055-457-3536 (C.M.)

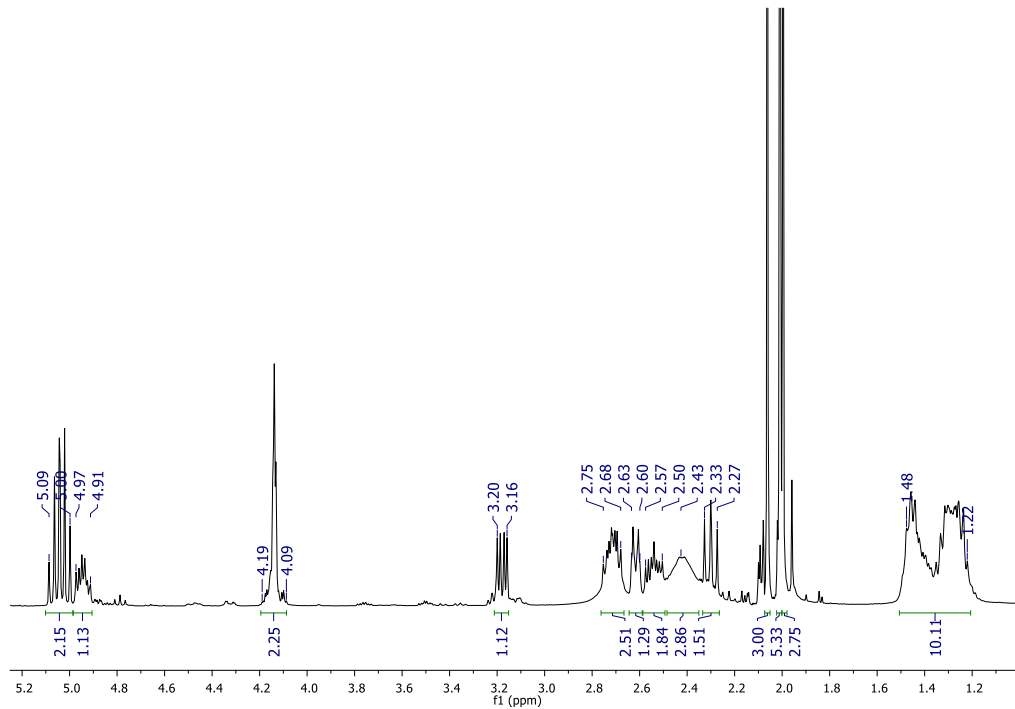
# Supplementary Materials

## Table of contents

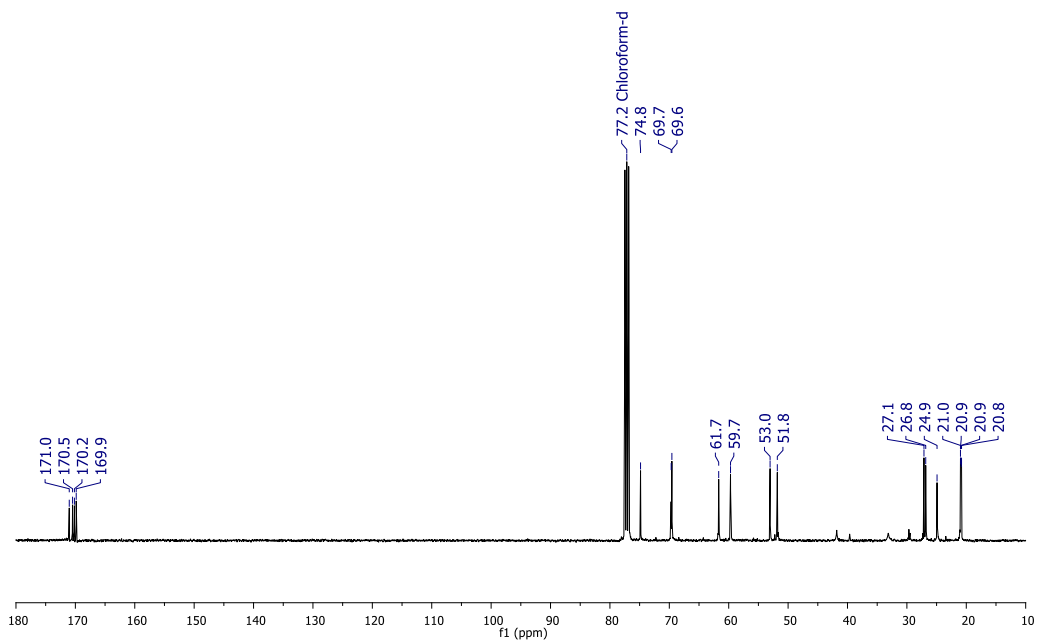
<sup>1</sup> H-NMR and <sup>13</sup> C-NMR spectra of compound <b>9</b> (Figures S1-S3)	S3
<sup>1</sup> H-NMR and <sup>13</sup> C-NMR spectra of compound <b>11</b> (Figures S4-S6)	S5
<sup>1</sup> H-NMR and <sup>13</sup> C-NMR spectra of compound <b>16</b> (Figures S7-S9)	S7
<sup>1</sup> H-NMR and <sup>13</sup> C-NMR spectra of compound <b>17</b> (Figures S10-S12)	S9
Characterization of AuGNP <b>1</b> (Figures S13-S16)	S11
Characterization of AuGNP <b>2</b> (Figures S17-S20)	S13
Characterization of AuGNP <b>3</b> (Figures S21-S24)	S15
Characterization of AuGNP <b>4</b> (Figures S25-S28)	S17
Characterization of AuGNP <b>5</b> (Figures S29-S32)	S19
Characterization Table for AuGNP <b>1-7</b> (Table S1)	S21
Inhibition assays of AuGNPs <b>1-5</b> (Figures S33-S37)	S23



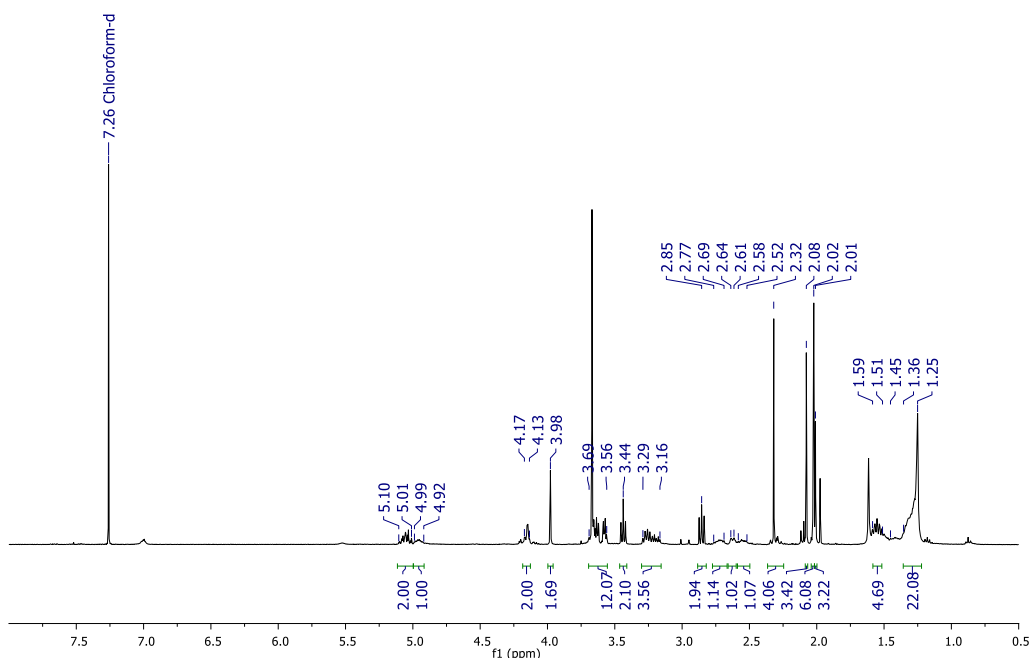
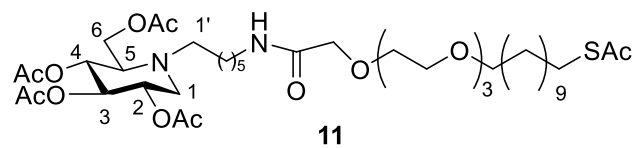
**Figure S1.** <sup>1</sup>H-NMR spectrum of compound **9** (400 MHz, CDCl<sub>3</sub>).



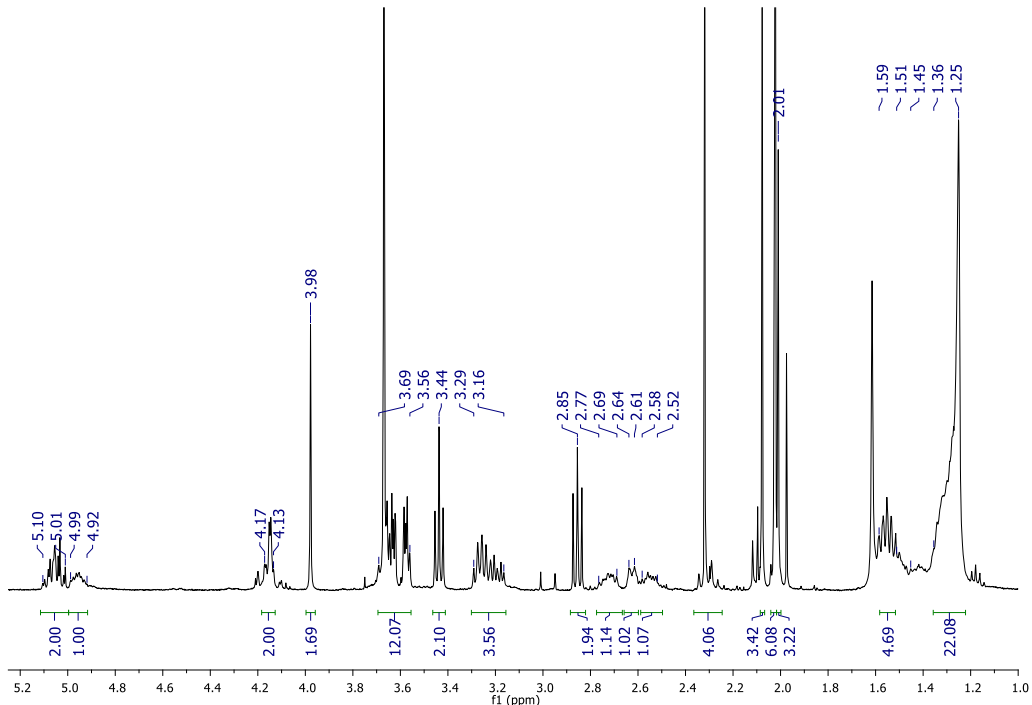
**Figure S2.** Expansion of <sup>1</sup>H-NMR spectrum of compound **9** (400 MHz, CDCl<sub>3</sub>).



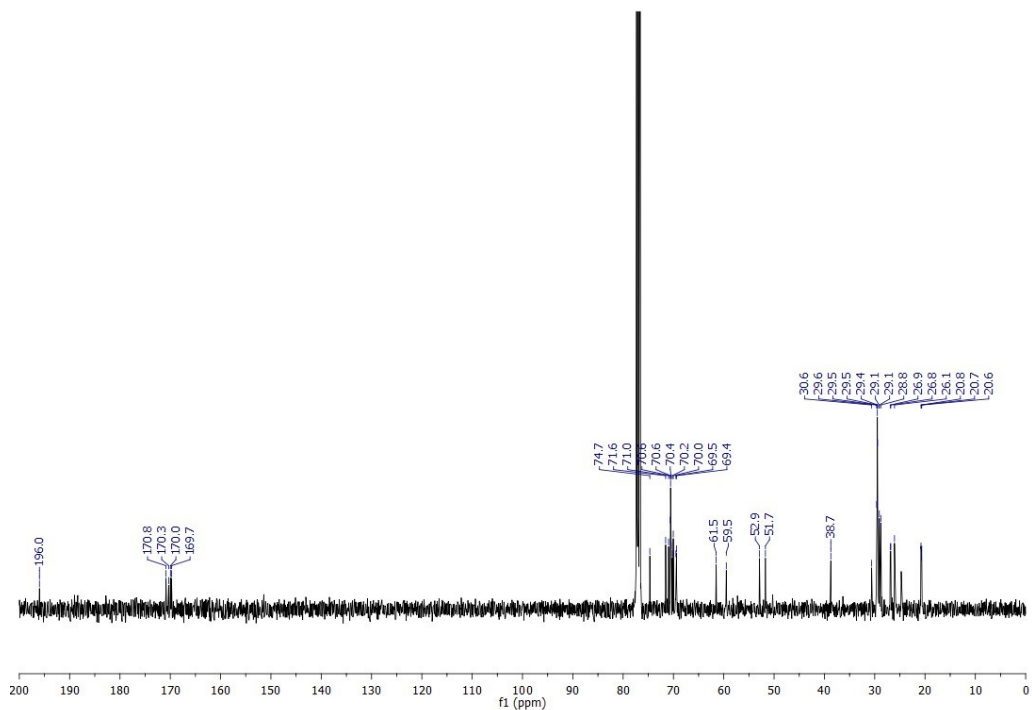
**Figure S3.**  $^{13}\text{C}$ -NMR spectrum of compound 9 (100 MHz,  $\text{CDCl}_3$ ).



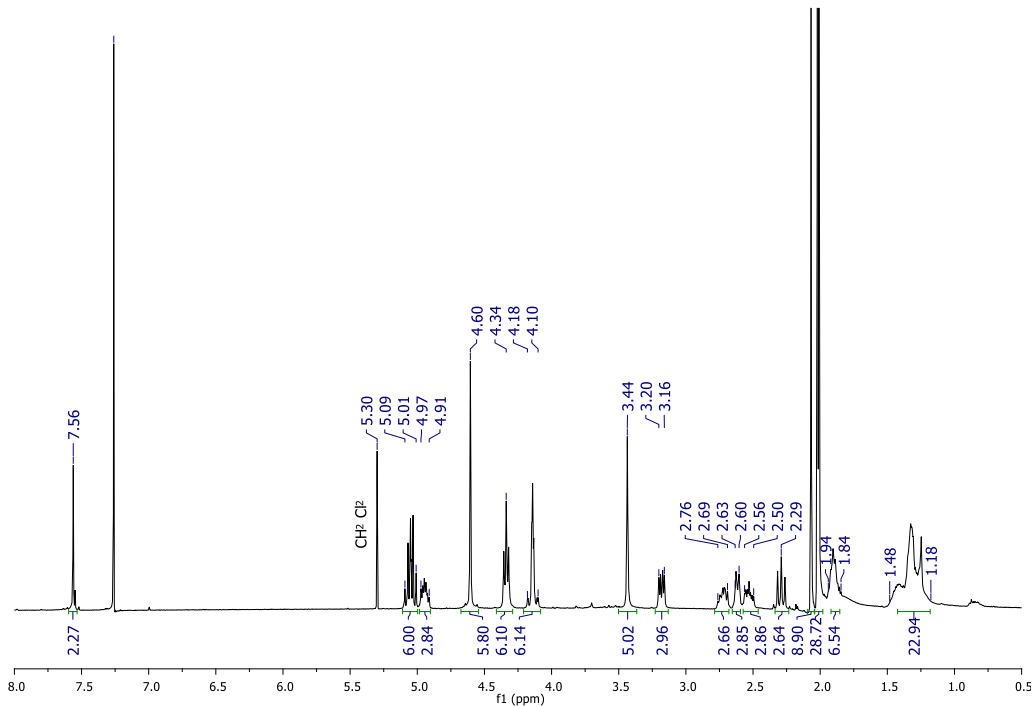
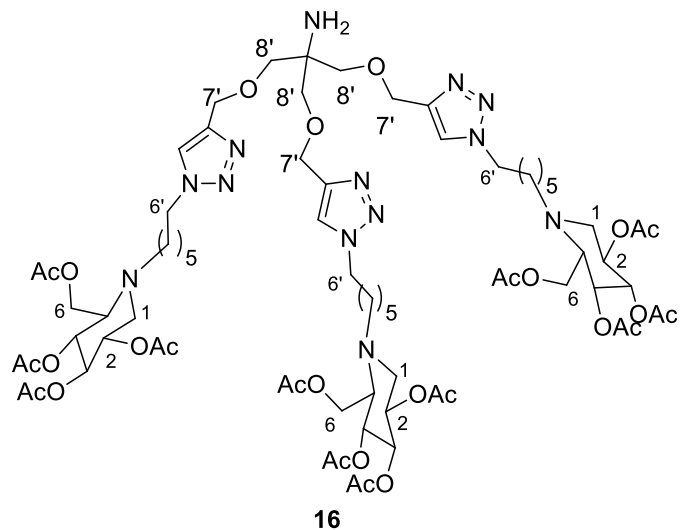
**Figure S4.**  $^1\text{H}$ -NMR spectrum of compound **11** (400 MHz,  $\text{CDCl}_3$ ).

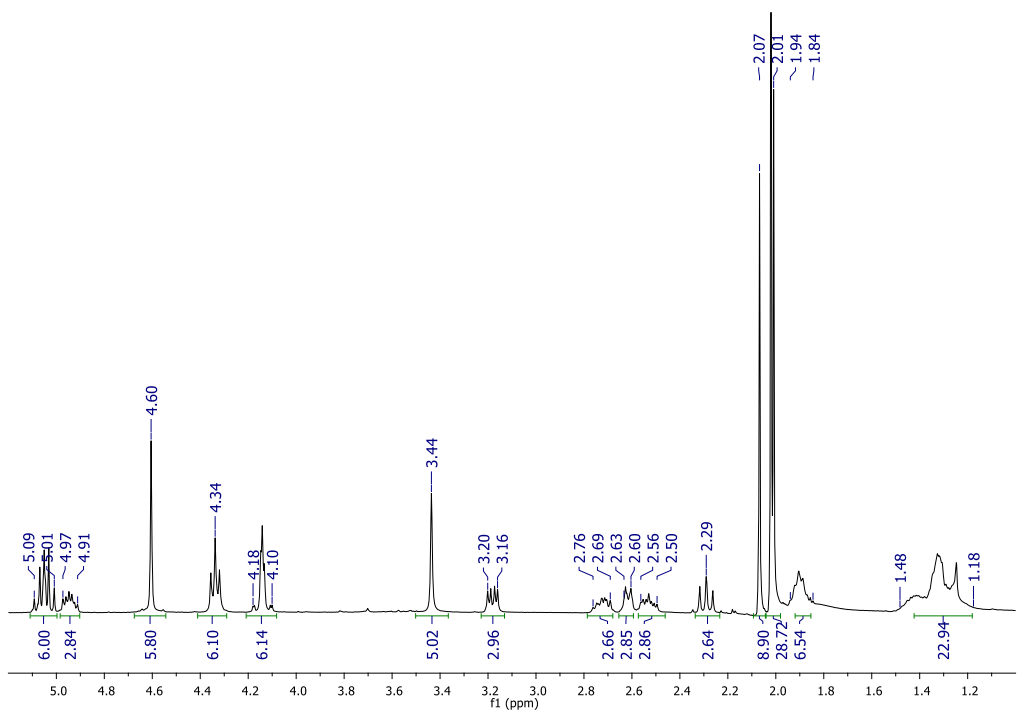


**Figure S5.** Expansion of  $^1\text{H}$ -NMR spectrum of compound **11** (400 MHz,  $\text{CDCl}_3$ ).

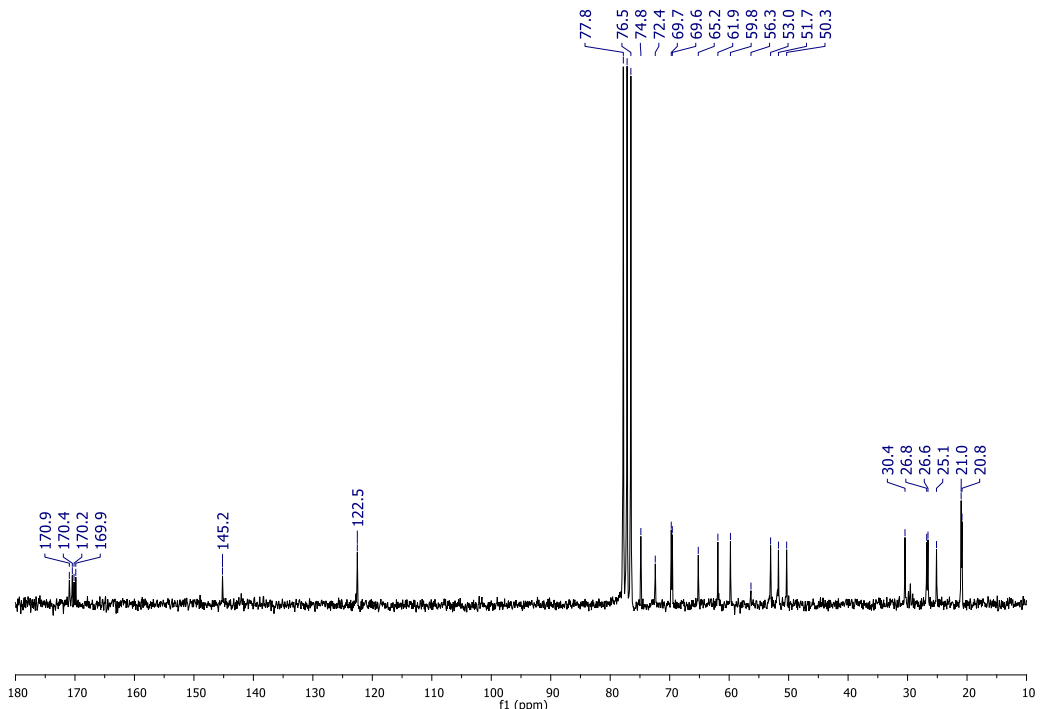


**Figure S6.** <sup>13</sup>C-NMR spectrum of compound **11** (100 MHz, CDCl<sub>3</sub>).

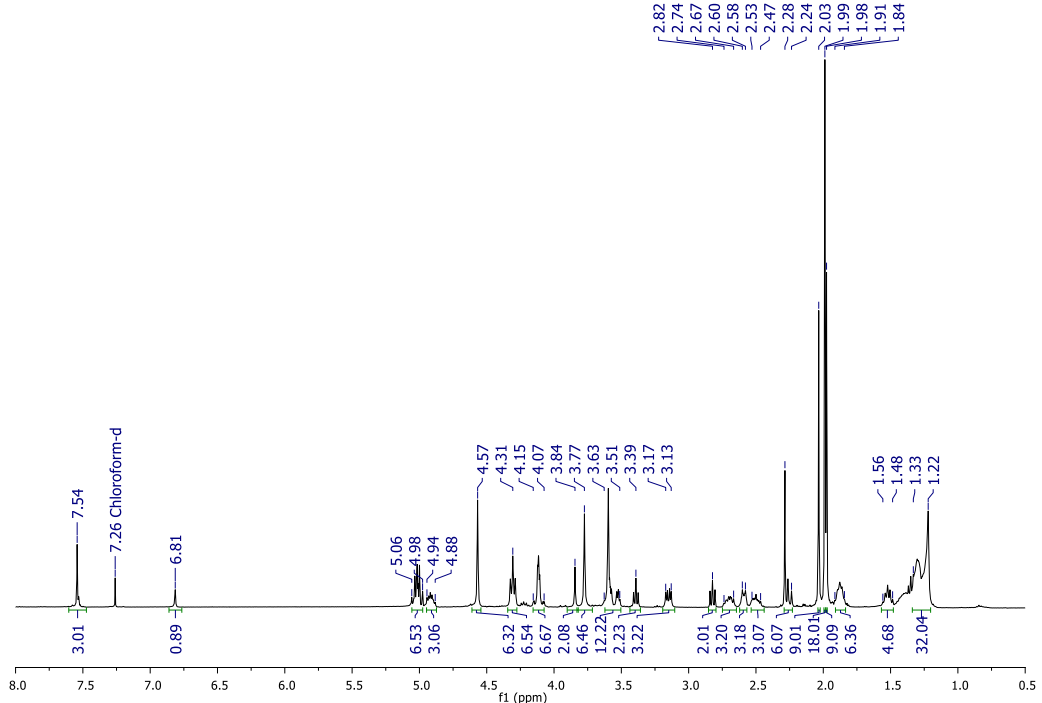
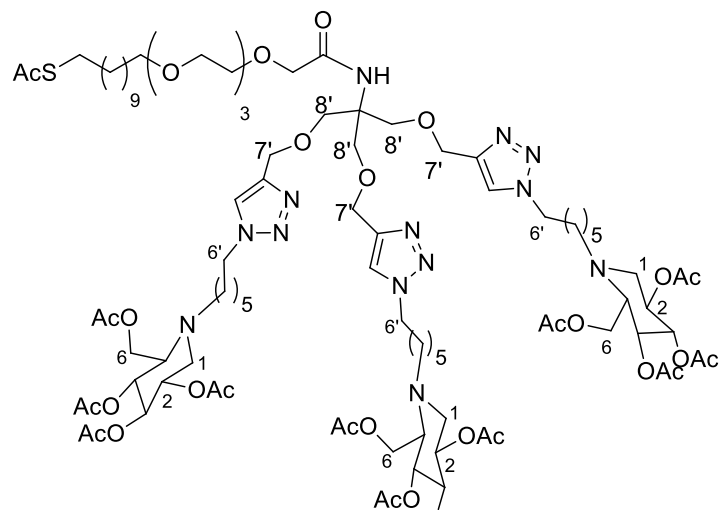




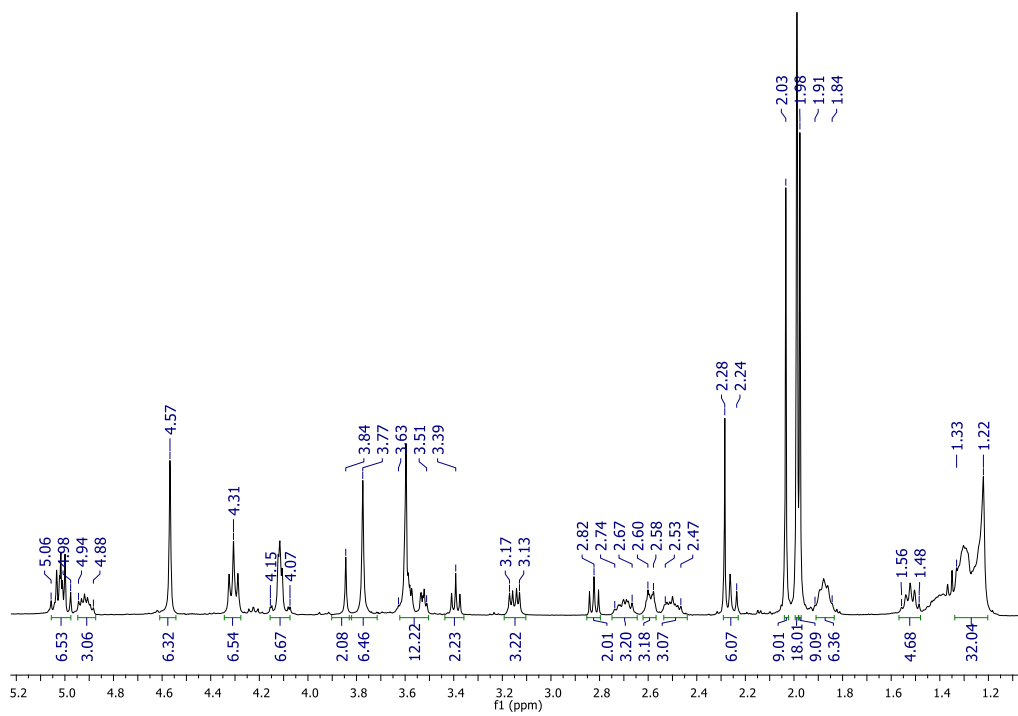
**Figure S8.** Expansion of <sup>1</sup>H-NMR spectrum of compound **16** (400 MHz, CDCl<sub>3</sub>).



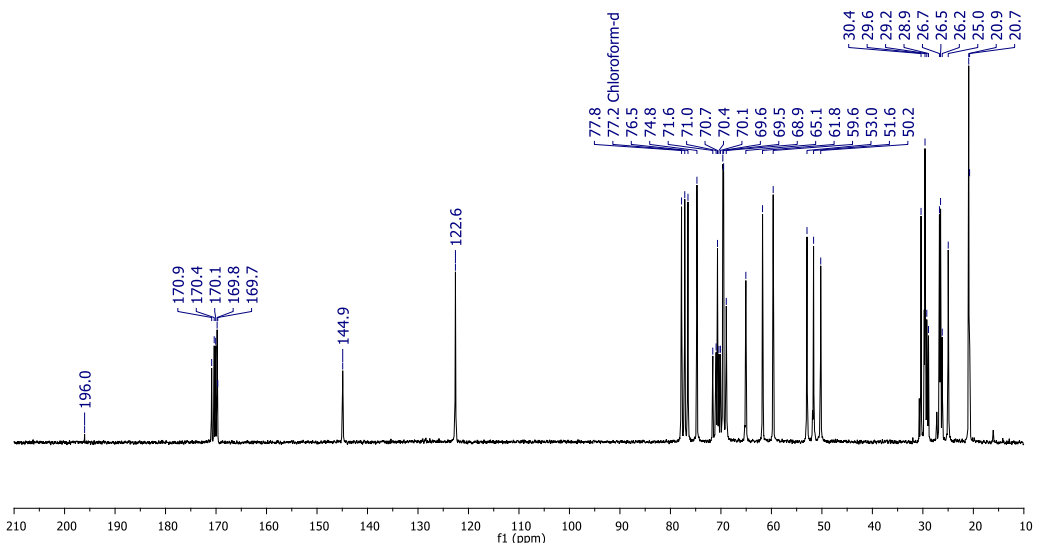
**Figure S9.** <sup>13</sup>C-NMR spectrum of compound **16** (100 MHz, CDCl<sub>3</sub>).



**Figure S10.**  $^1\text{H}$ -NMR spectrum of compound **17** (400 MHz,  $\text{CDCl}_3$ ).

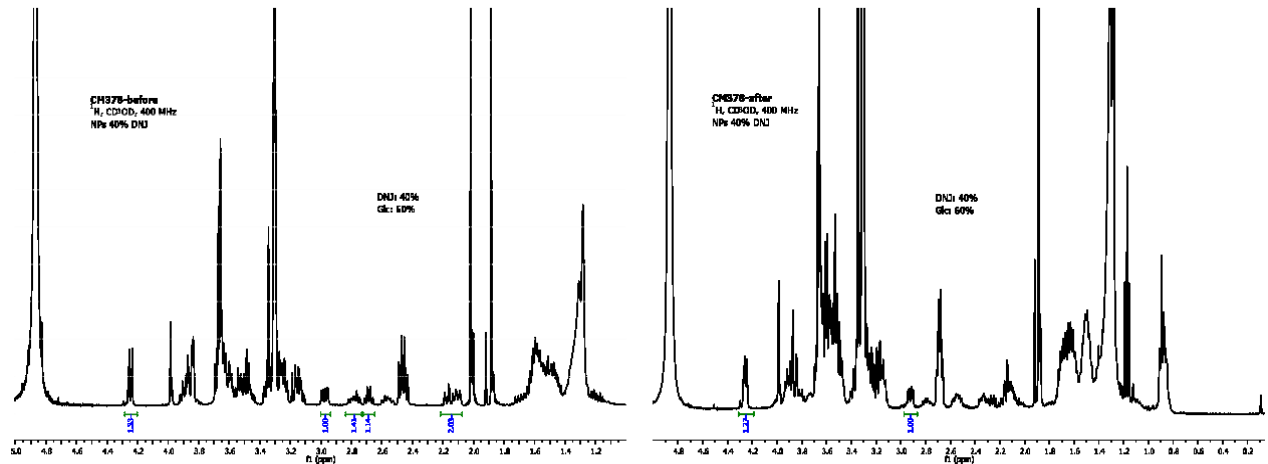


**Figure S11.** Expansion of  $^1\text{H}$ -NMR spectrum of compound **17** (400 MHz,  $\text{CDCl}_3$ ).

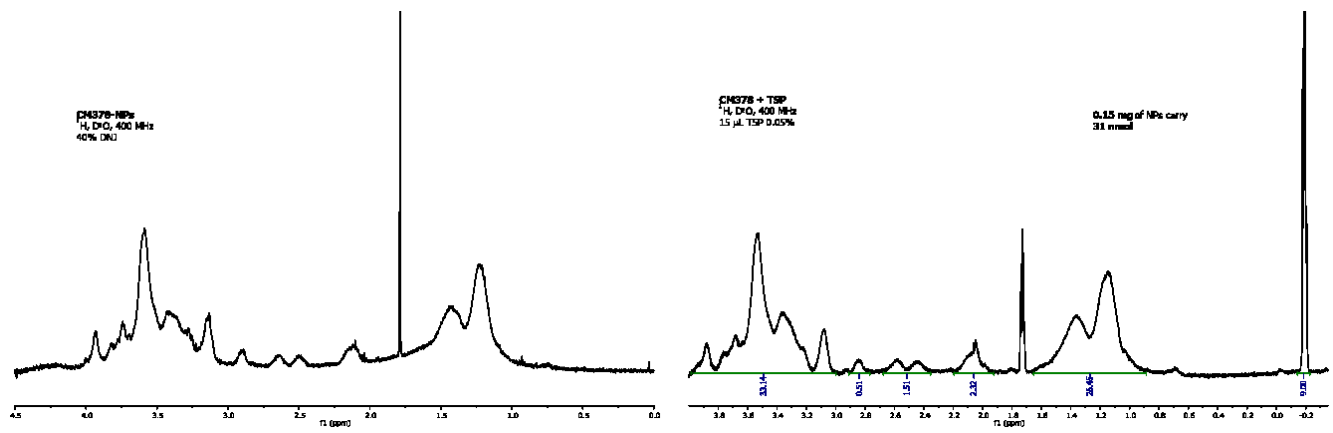


**Figure S12.**  $^{13}\text{C}$ -NMR spectrum of compound **17** (100 MHz,  $\text{CDCl}_3$ ).

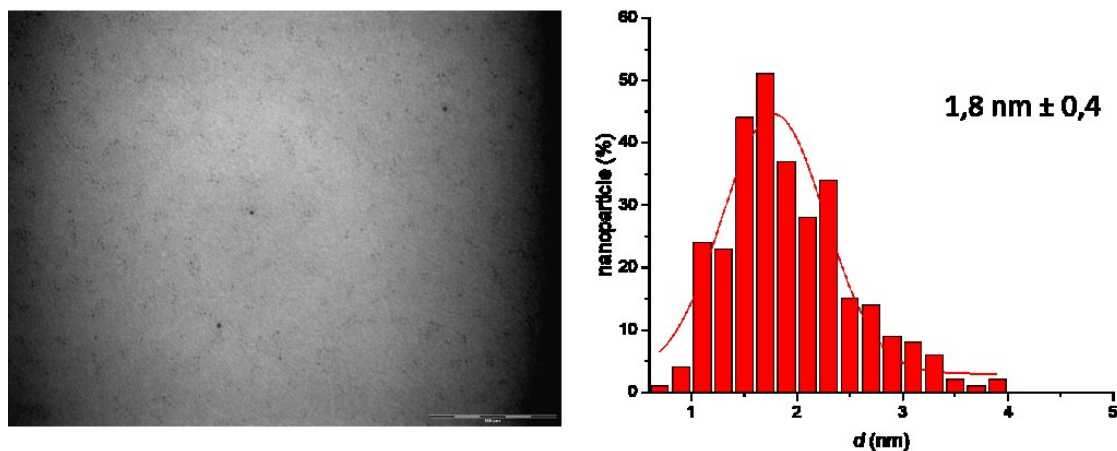
*Characterization of AuGNP 1*



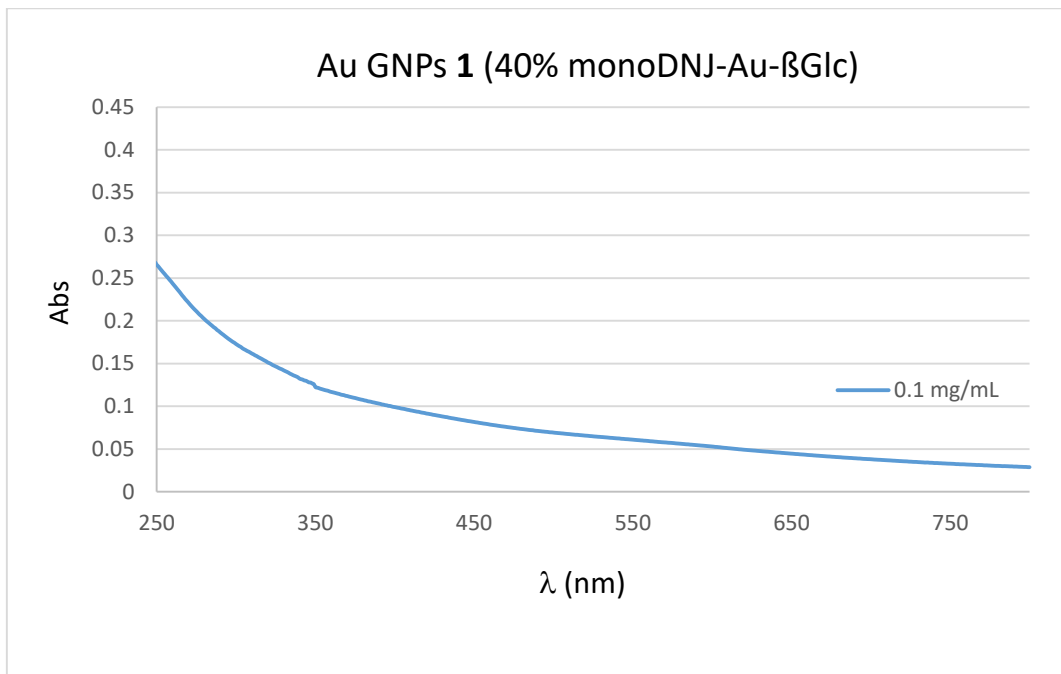
**Figure S13.** <sup>1</sup>H NMR of sugar/iminosugar ligands mixture before (left) and after (right) formation of AuGNP 1 (400 MHz, CD<sub>3</sub>OD).



**Figure S14.** <sup>1</sup>H NMR and <sup>1</sup>H qNMR with TSP-d<sub>4</sub> of AuGNP 1 (400 MHz, D<sub>2</sub>O).

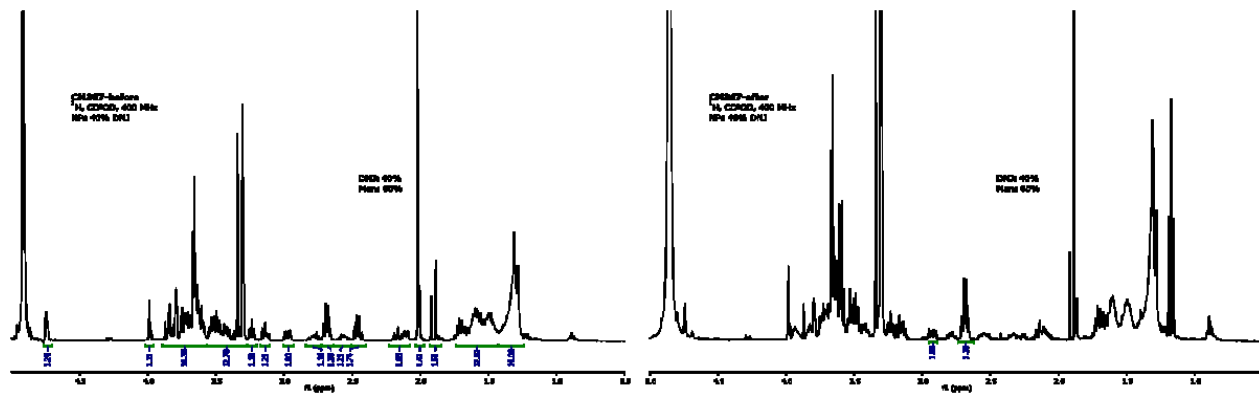


**Figure S15.** TEM micrograph (scale = 100 nm) in H<sub>2</sub>O and size-distribution histogram obtained by measuring 300 nanoparticles of AuGNP **1** (average diameter:  $1.8 \pm 0.4$  nm).

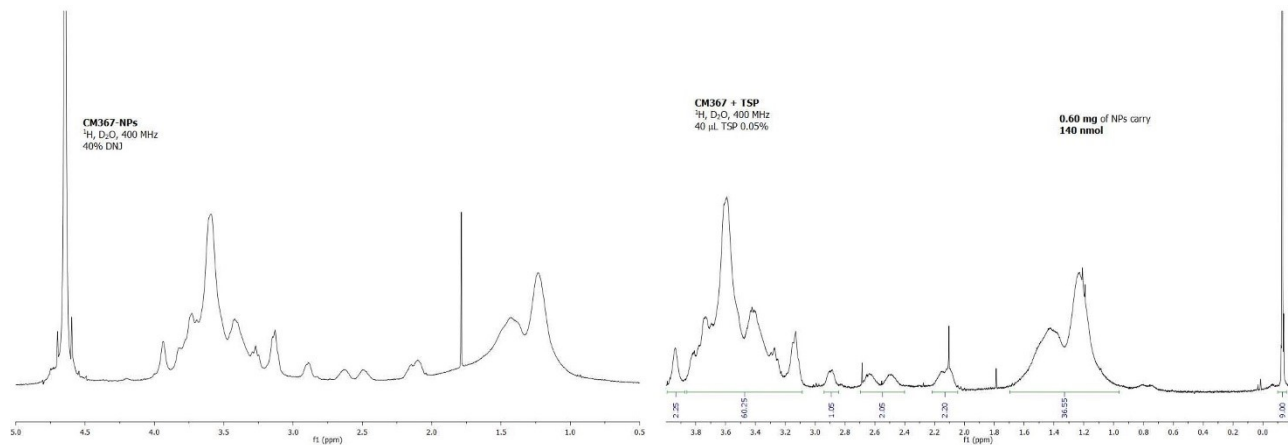


**Figure S16.** UV/vis spectrum of H<sub>2</sub>O solution of AuGNP **1** recorded at concentration of 0.1 mg/mL.

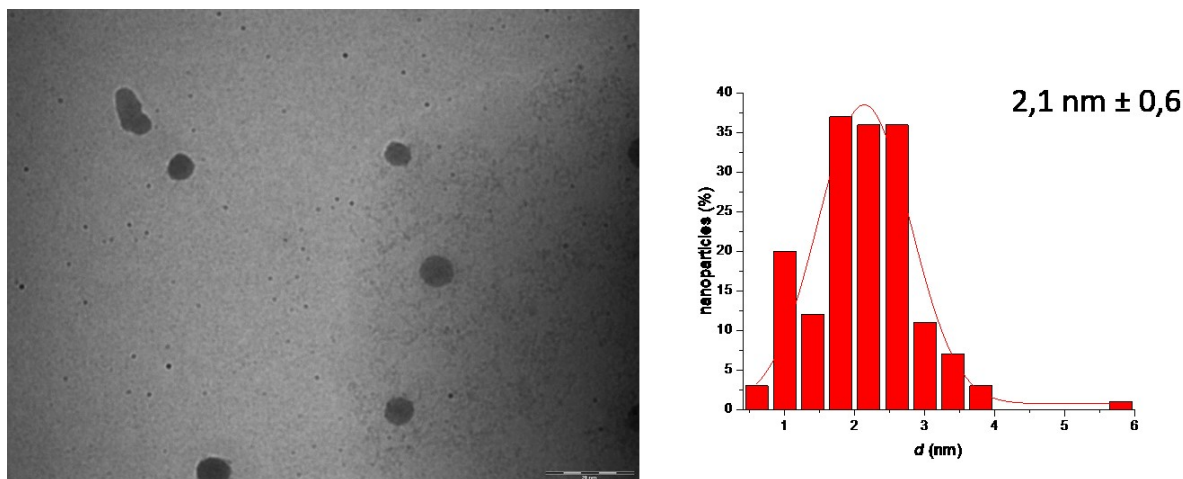
*Characterization of AuGNP 2*



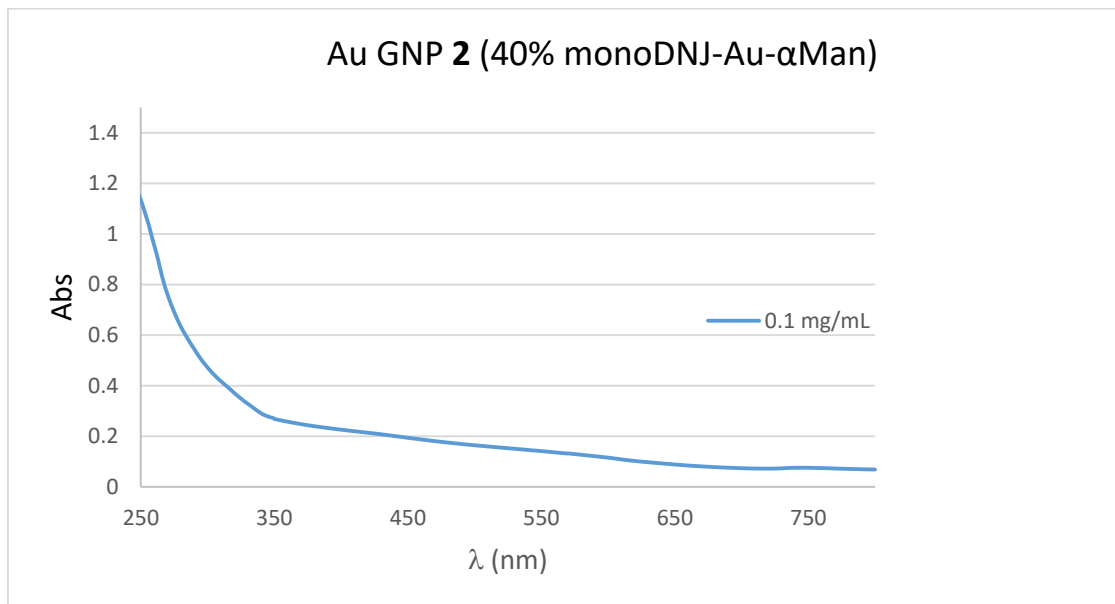
**Figure S17.** <sup>1</sup>H NMR of sugar/iminosugar ligands mixture before (left) and after (right) formation of AuGNP 2 (400 MHz,  $\text{CD}_3\text{OD}$ ).



**Figure S18.** <sup>1</sup>H NMR and <sup>1</sup>H qNMR with TSP-d<sub>4</sub> of AuGNP 2 (400 MHz,  $\text{D}_2\text{O}$ ).

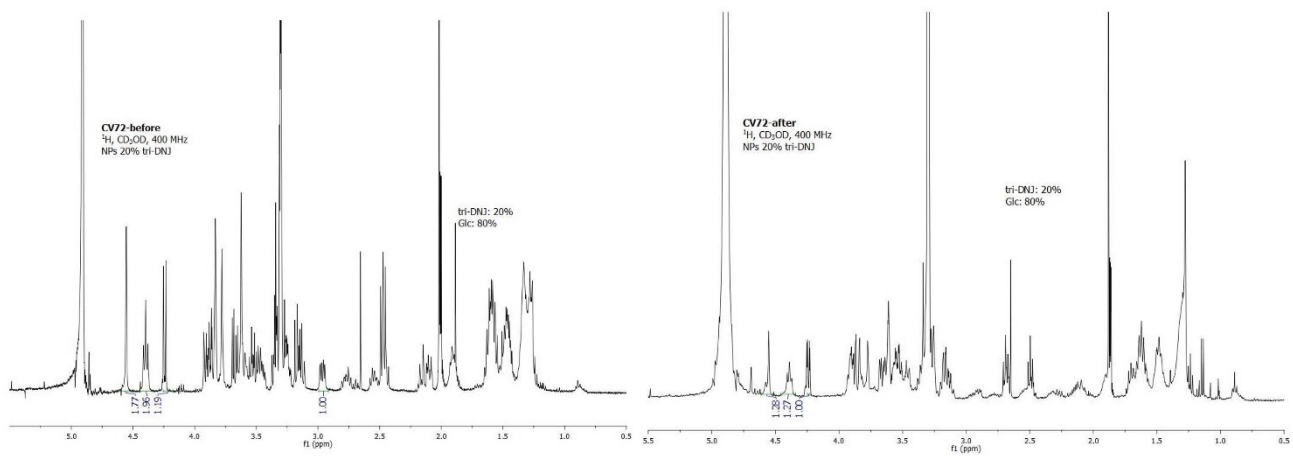


**Figure S19.** TEM micrograph (scale = 20 nm) in H<sub>2</sub>O and size-distribution histogram obtained by measuring 300 nanoparticles of AuGNP **2** (average diameter: 2.1 ±0.6 nm, less than 3% shows a >5 nm diameter).

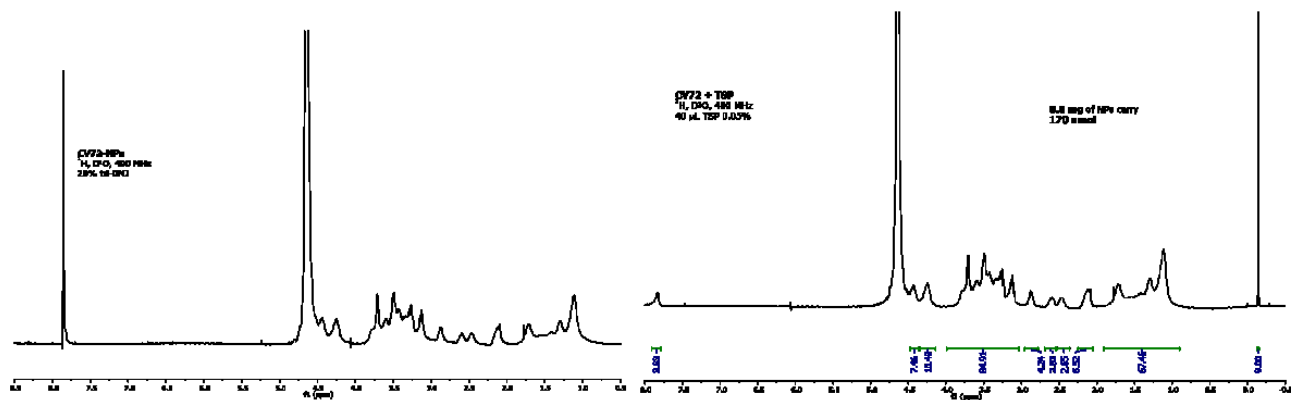


**Figure S20.** UV/vis spectrum of H<sub>2</sub>O solution of AuGNP **2** recorded at concentration of 0.1 mg/mL.

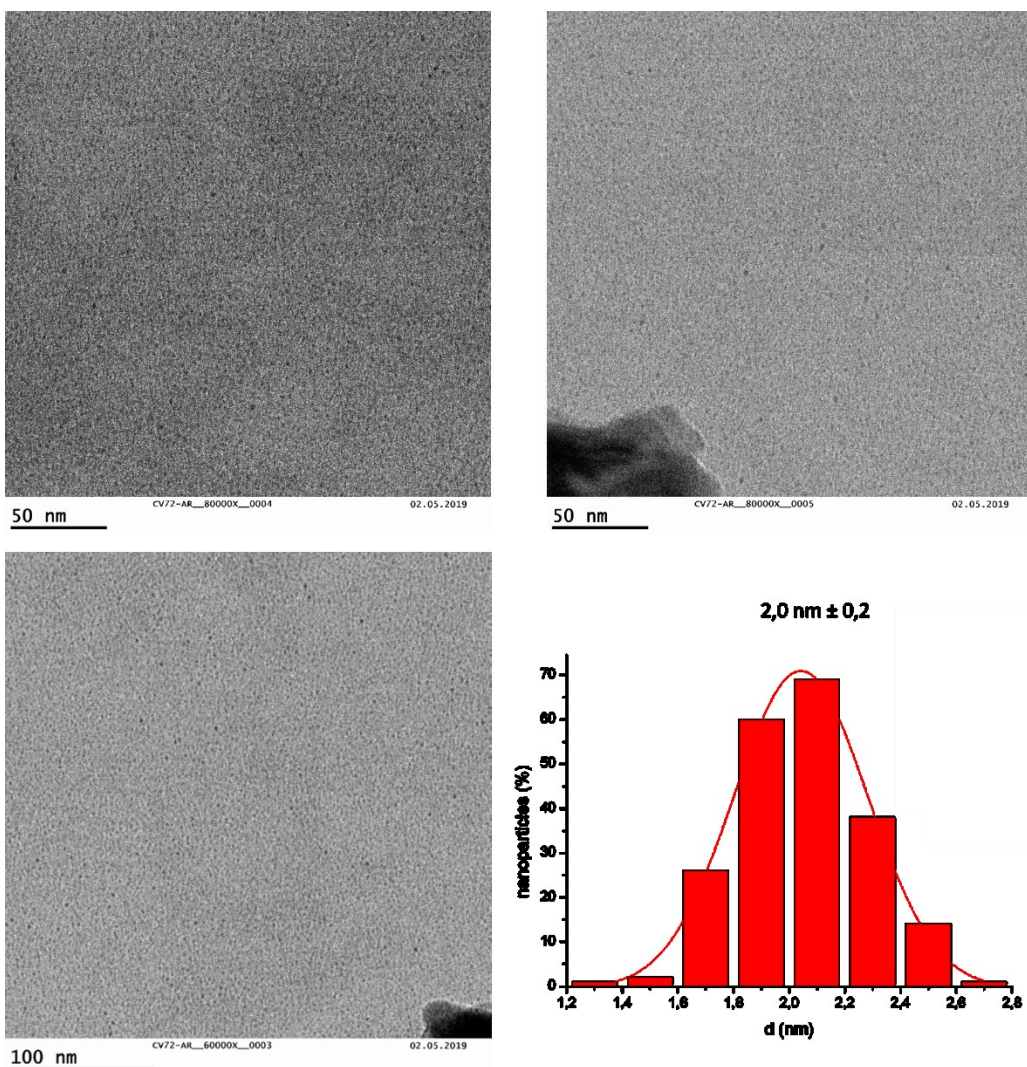
*Characterization of AuGNP 3*



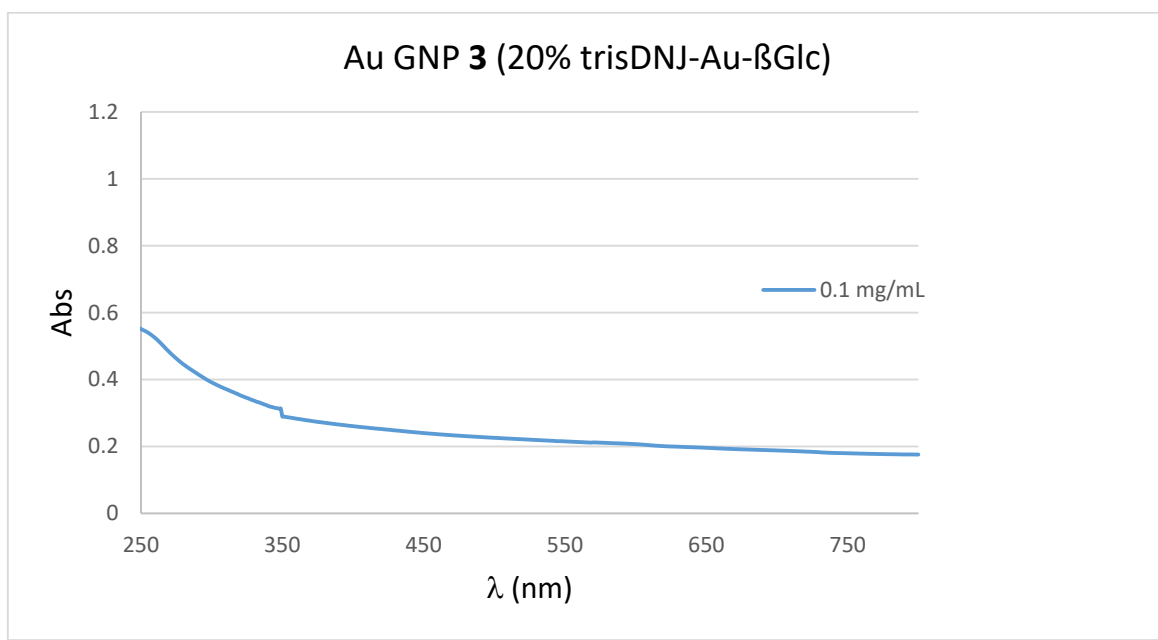
**Figure S21.** <sup>1</sup>H NMR of sugar/iminosugar ligands mixture before (left) and after (right) formation of AuGNP 3 (400 MHz, CD<sub>3</sub>OD).



**Figure S22.** <sup>1</sup>H NMR and <sup>1</sup>H qNMR with TSP-d<sub>4</sub> of AuGNP 3 (400 MHz, D<sub>2</sub>O).

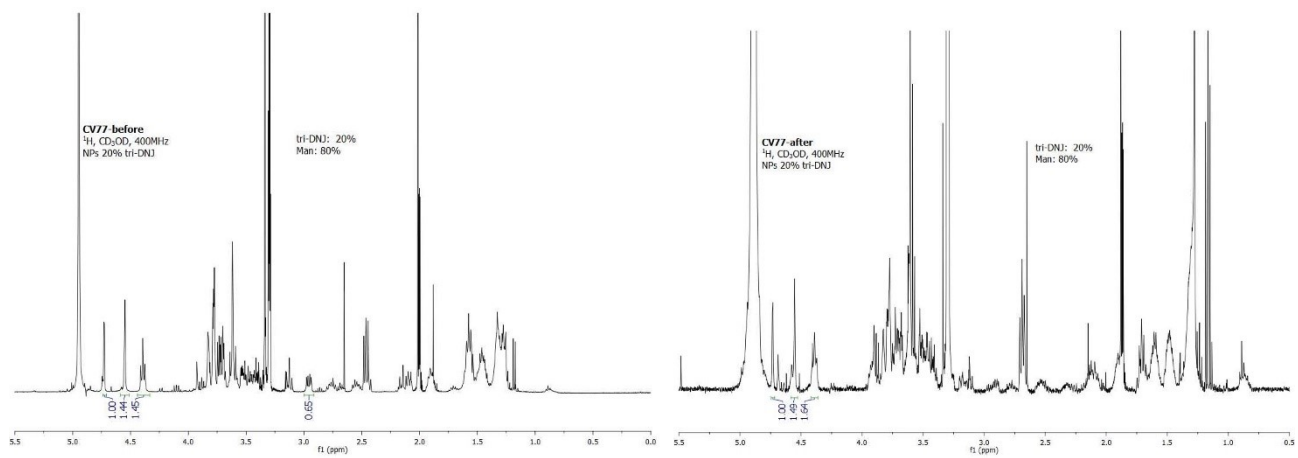


**Figure S23.** TEM micrographs in H<sub>2</sub>O (magnification 80000x and 60000x) and size-distribution histogram obtained by measuring 300 nanoparticles of AuGNP **3** (average diameter:  $2.1 \pm 0.5 \text{ nm}$ ).

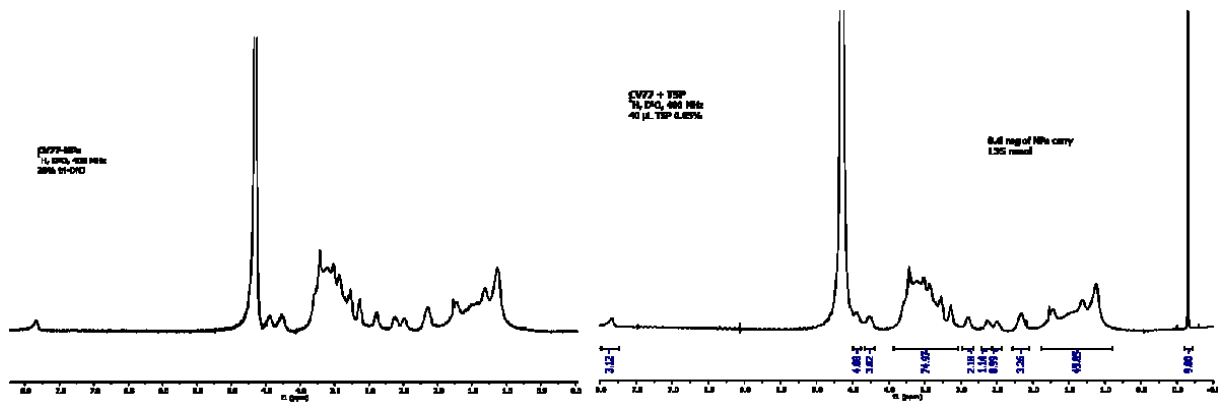


**Figure S24.** UV/vis spectrum of H<sub>2</sub>O solution of AuGNP **3** recorded at concentration of 0.1 mg/mL.

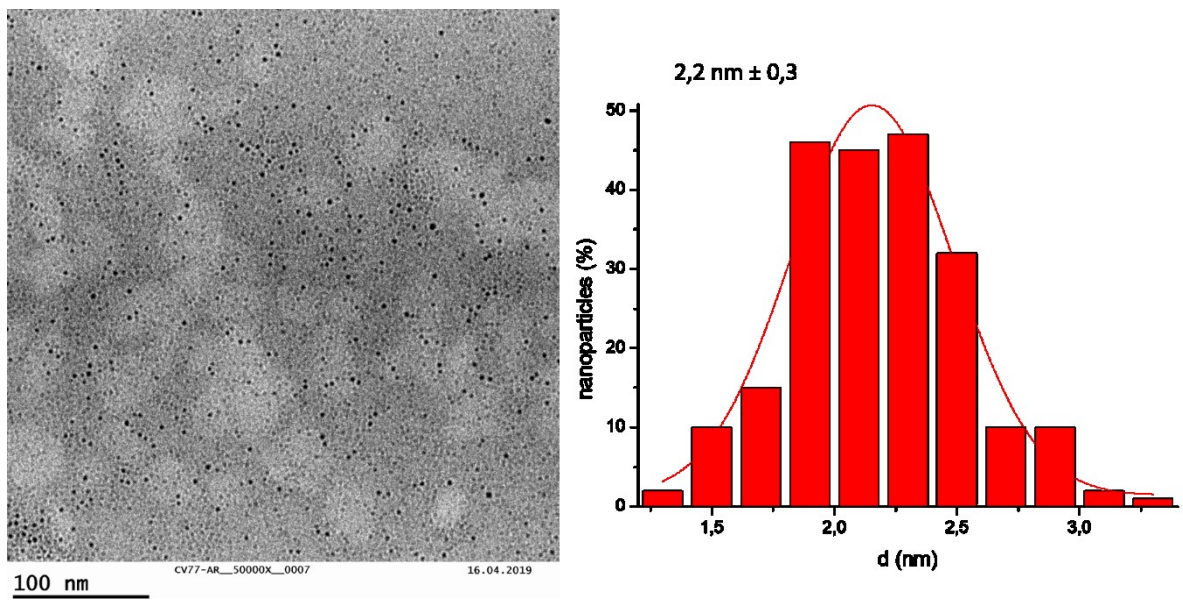
*Characterization of AuGNP 4*



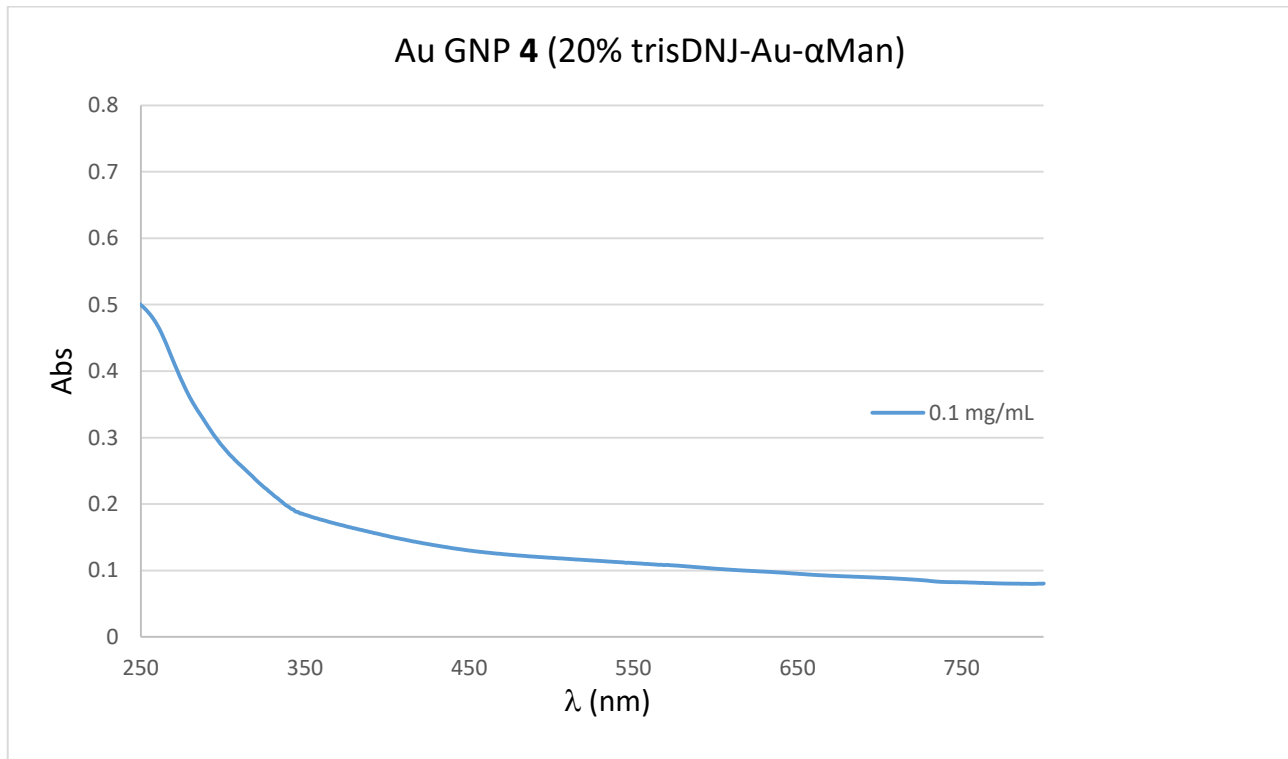
**Figure S25.** <sup>1</sup>H NMR of sugar/iminosugar ligands mixture before (left) and after (right) formation of AuGNP 4 (400 MHz, CD<sub>3</sub>OD).



**Figure S26.** <sup>1</sup>H NMR and <sup>1</sup>H qNMR with TSP-d<sub>4</sub> of AuGNP 4 (400 MHz, D<sub>2</sub>O).

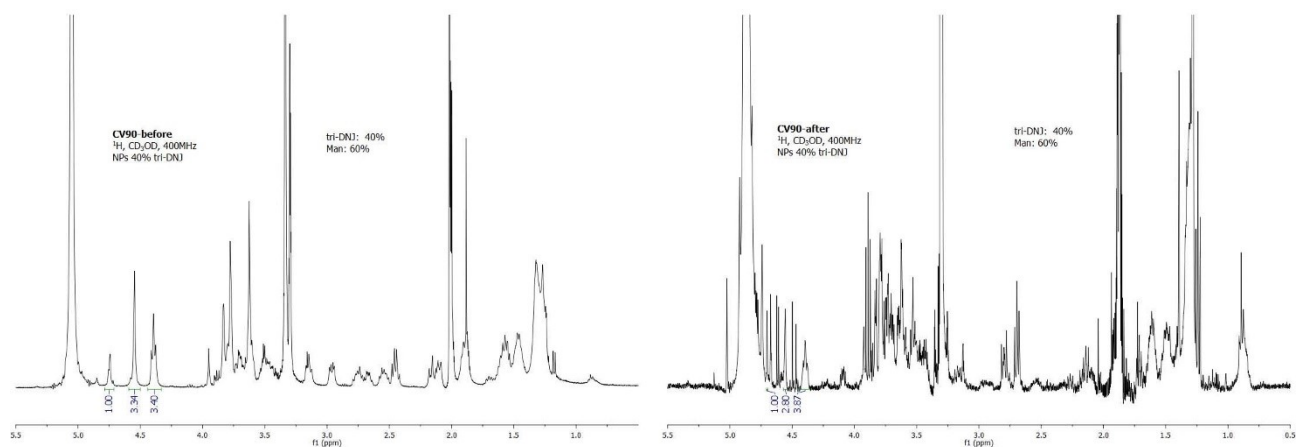


**Figure S27.** TEM micrograph in H<sub>2</sub>O and size-distribution histogram obtained by measuring 300 nanoparticles of AuGNP **4** (average diameter: 2.0 ± 0.4 nm).

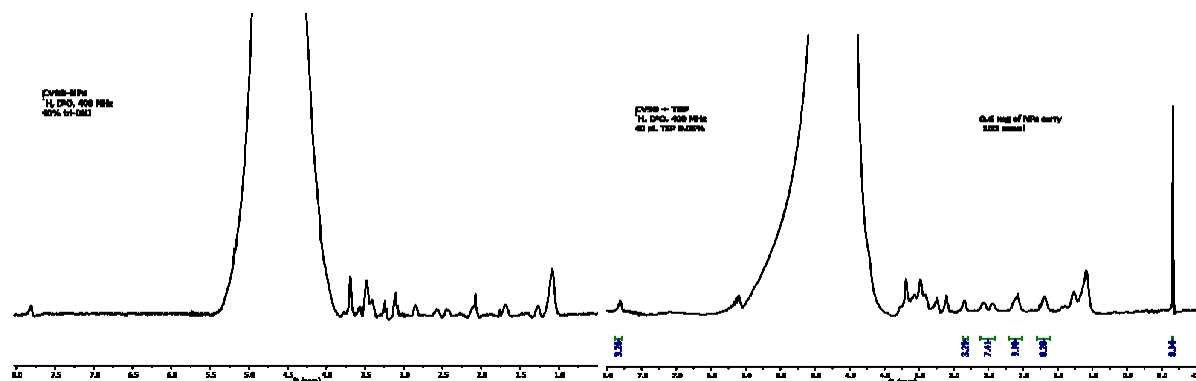


**Figure S28.** UV/vis spectrum of H<sub>2</sub>O solution of AuGNP **4** recorded at concentration of 0.1 mg/mL.

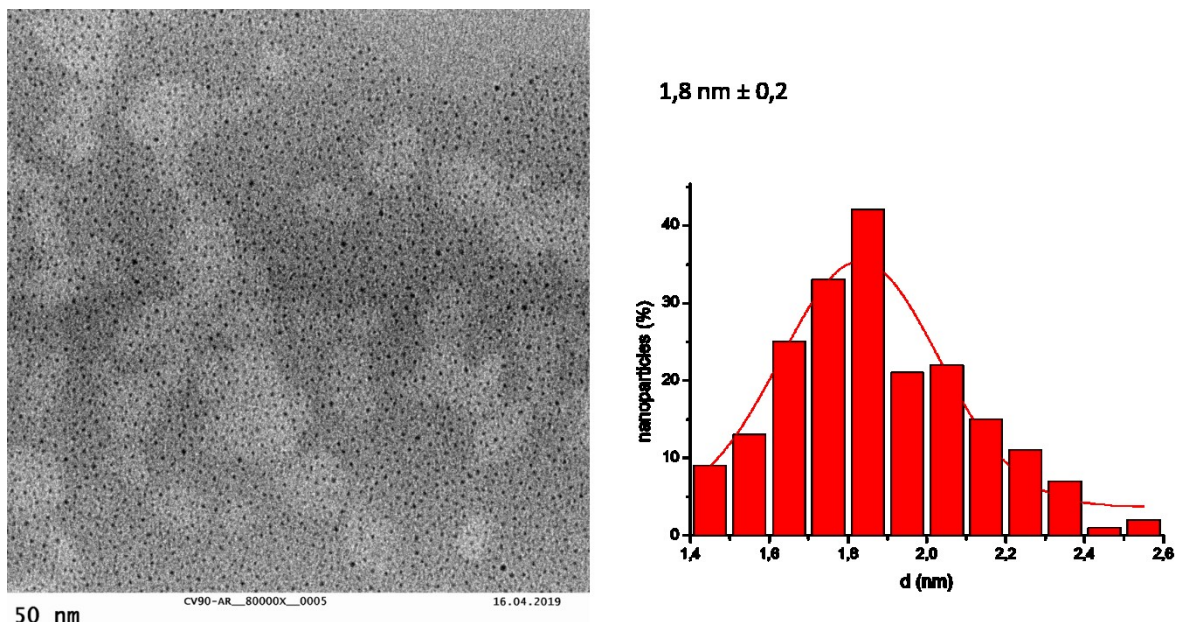
*Characterization of AuGNP 5*



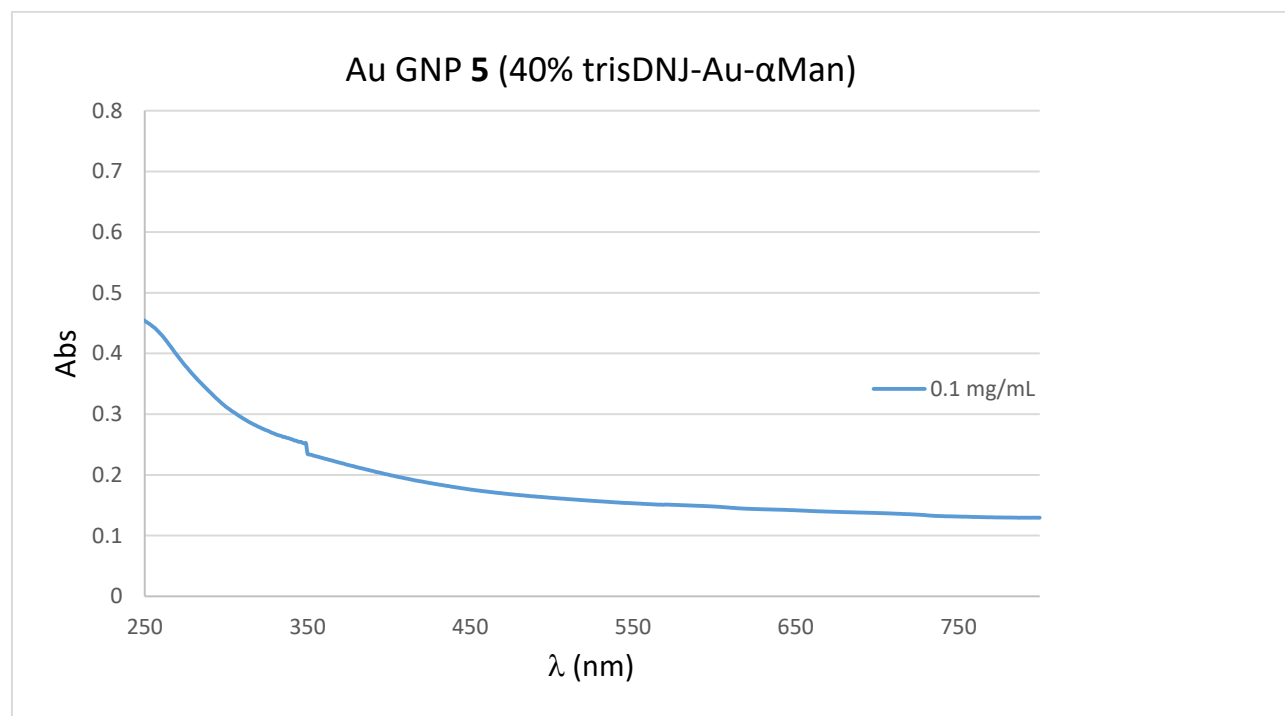
**Figure S29.** <sup>1</sup>H NMR of sugar/iminosugar ligands mixture before (left) and after (right) formation of AuGNP 5 (400 MHz, CD<sub>3</sub>OD).



**Figure S30.** <sup>1</sup>H NMR and <sup>1</sup>H qNMR with TSP-d<sub>4</sub> of AuGNP 5 (400 MHz, D<sub>2</sub>O).

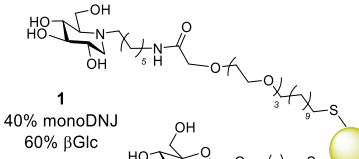
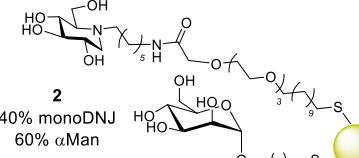
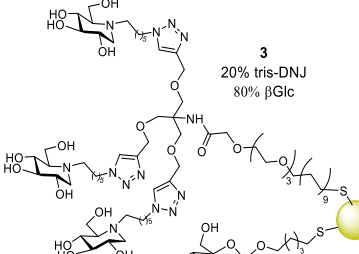
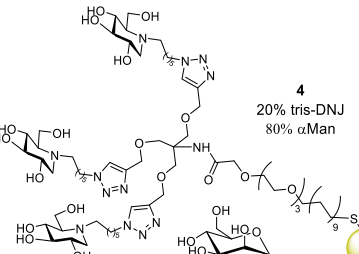


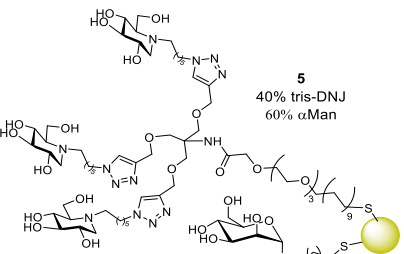
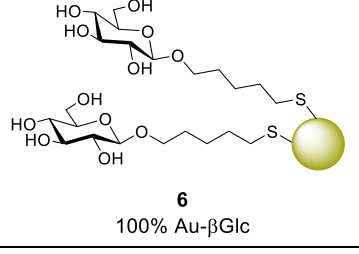
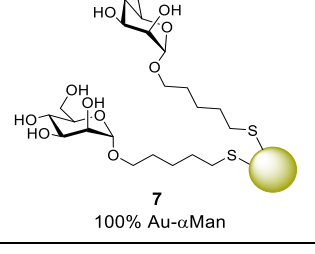
**Figure S31.** TEM micrograph in H<sub>2</sub>O and size-distribution histogram obtained by measuring 300 nanoparticles of AuGNP **5** (average diameter: 2.1 ± 0.5 nm).



**Figure S32.** UV/vis spectrum of H<sub>2</sub>O solution of AuGNP **5** recorded at concentration of 0.1 mg/mL.

**Table S1.** Summary table of DNJ-based AuGNPs **1-7** and their characterization.

Au-GNPs <sup>[1]</sup>	Characterization	
	Gold core size <sup>[2]</sup>	DNJ concentration for 2 mg/mL concentration of AuGPN <sup>[3]</sup>
 <b>1</b> 40% monoDNJ 60% $\beta$ Glc	1.8±0.4 nm	413 $\mu$ M
 <b>2</b> 40% monoDNJ 60% $\alpha$ Man	2.1±0.6 nm	467 $\mu$ M
 <b>3</b> 20% tris-DNJ 80% $\beta$ Glc	2.1±0.5 nm	567 $\mu$ M
 <b>4</b> 20% tris-DNJ 80% $\alpha$ Man	2.0±0.4 nm	450 $\mu$ M

 <p>5 40% tris-DNJ 60% <math>\alpha</math>Man</p>	$2.1 \pm 0.5$ nm	503 $\mu$ M
 <p>6 100% Au-<math>\beta</math>Glc</p>	$1.7 \pm 0.4$ nm	/
 <p>7 100% Au-<math>\alpha</math>Man</p>	$1.6 \pm 0.4$ nm	/

[1] The given percentages refer to the proportion of the ligands on the gold surface as determined by recording  $^1\text{H}$  NMR spectrum of their initial mixture before the formation of the AuGNPs and confirmed by  $^1\text{H}$  NMR spectrum of the supernatant after the AuGNPs formation. [2] Determined by Transmission Electron Microscopy (TEM). [3] Determined on the basis of qNMR analysis.

*Inhibition assays*

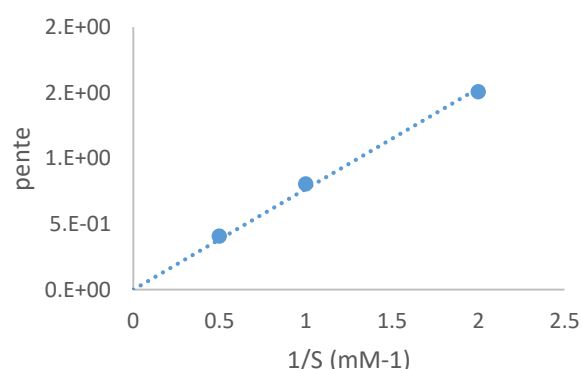
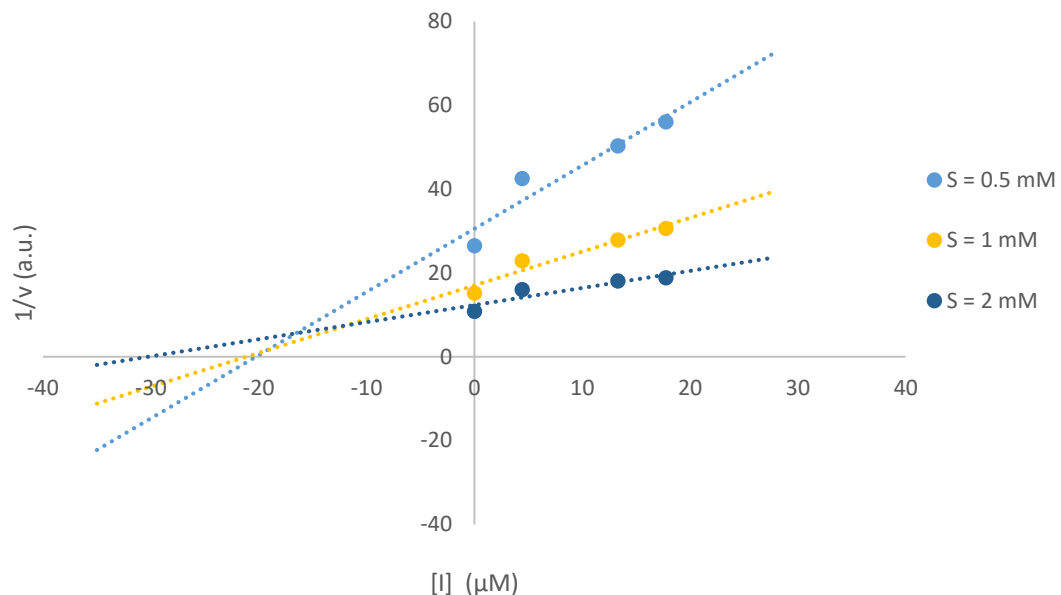


**Figure S33.** Dixon plot for  $K_i$  determination of compound AuGNP **1** against JB $\alpha$ -man and replot of the slopes showing competitive mode.  $K_i = 16 \pm 2 \mu\text{M}$ .

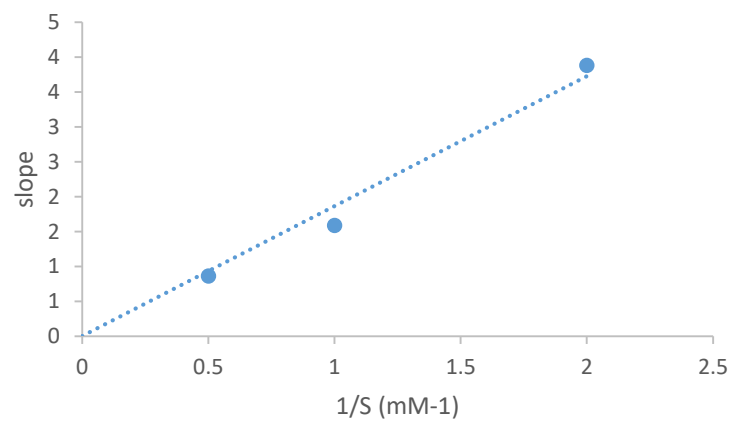
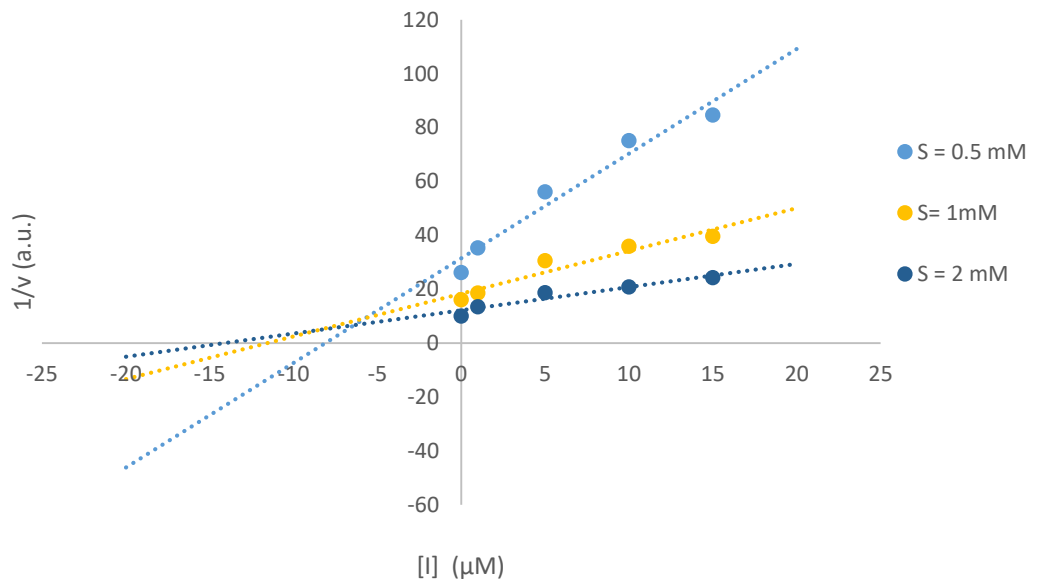


**Figure S34.** Dixon plot for  $K_i$  determination of compound AuGNP **2** against JB $\alpha$ -man and replot of the slopes showing competitive mode.  $K_i = 8 \pm 2 \mu\text{M}$ .

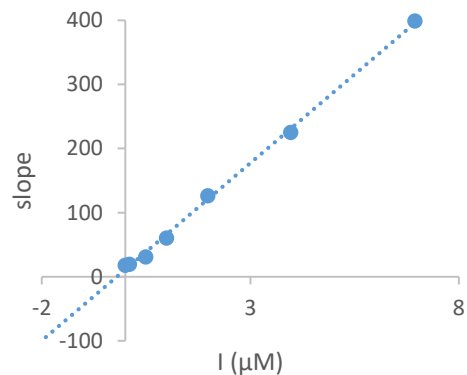
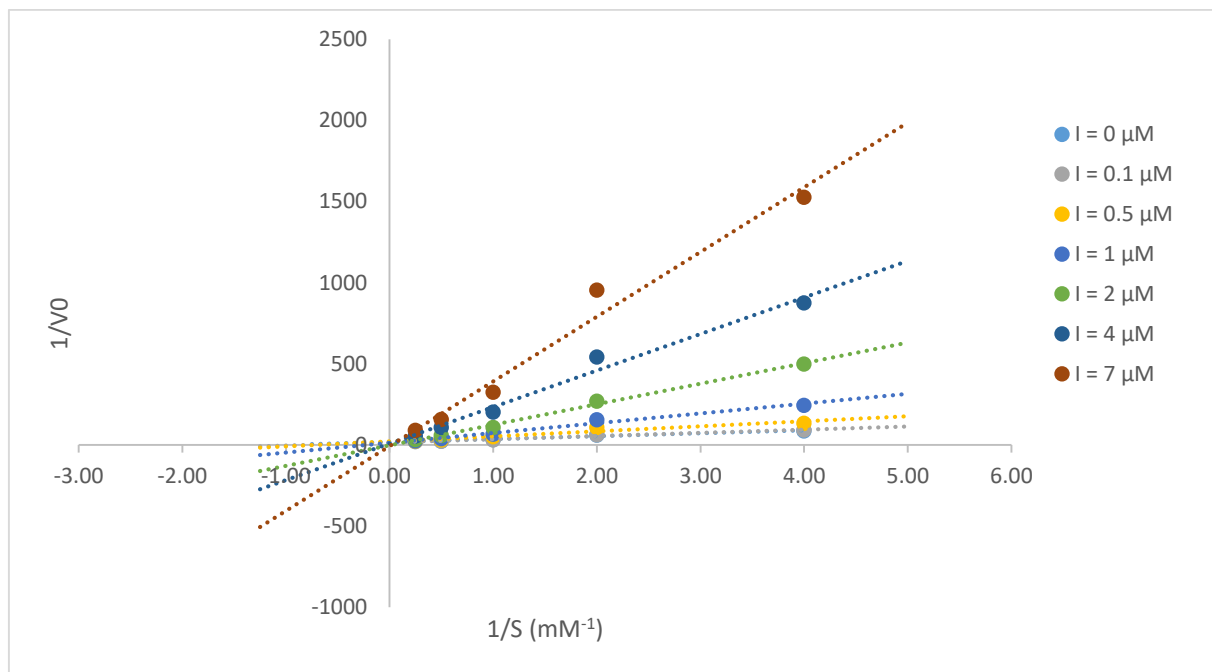


**Figure S35.** Lineweaver-Burk plots and replot of the slope versus inhibitor concentration for  $K_i$  determination of compound AuGnP **3** against JB $\alpha$ -man.

$$K_i = 0.198 \pm 0.060 \mu\text{M}.$$

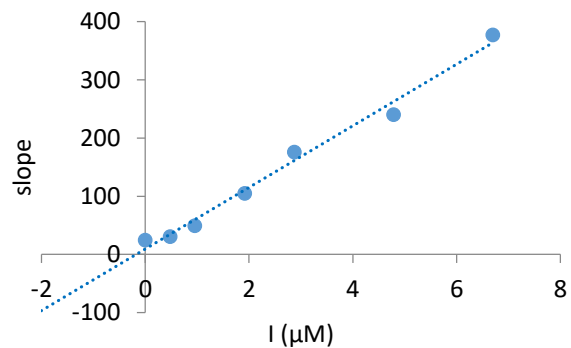
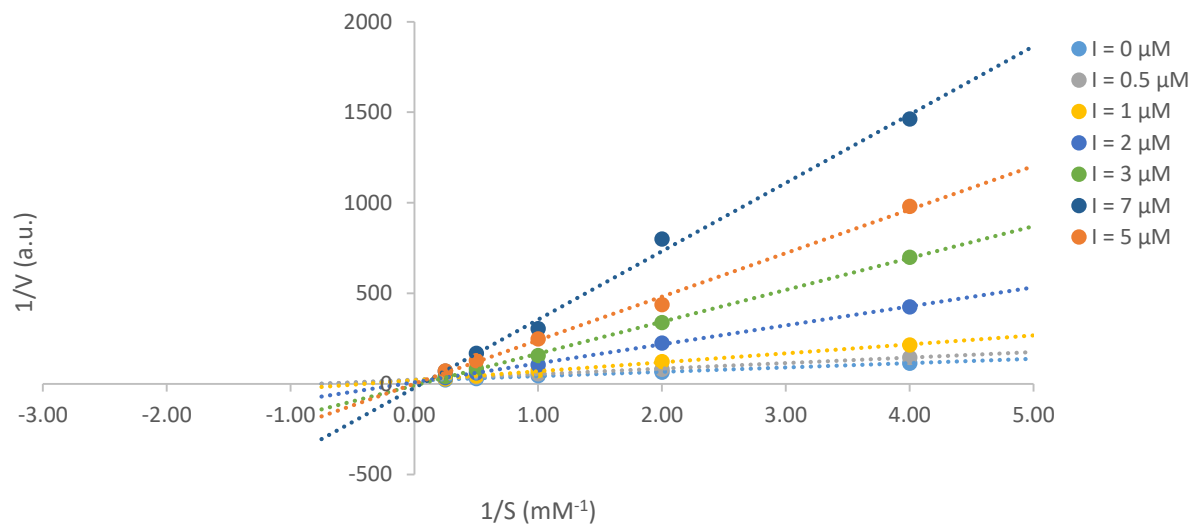


**Figure S36.** Lineweaver-Burk plots and replot of the slope versus inhibitor concentration for  $K_i$  determination of compound AuGnP 4 against JB $\alpha$ -man.

$$K_i = 0.175 \pm 0.171 \mu\text{M}.$$

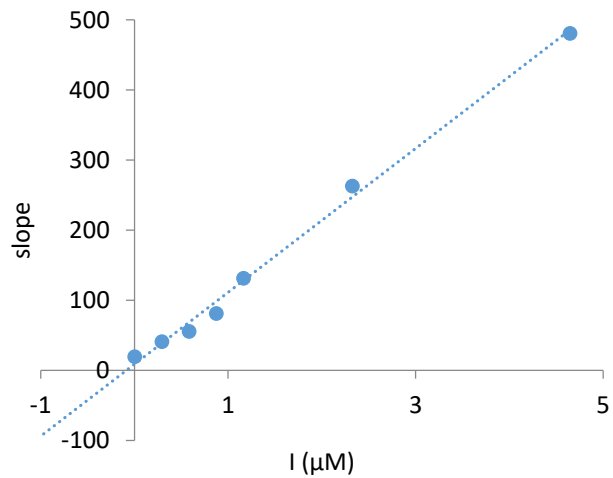
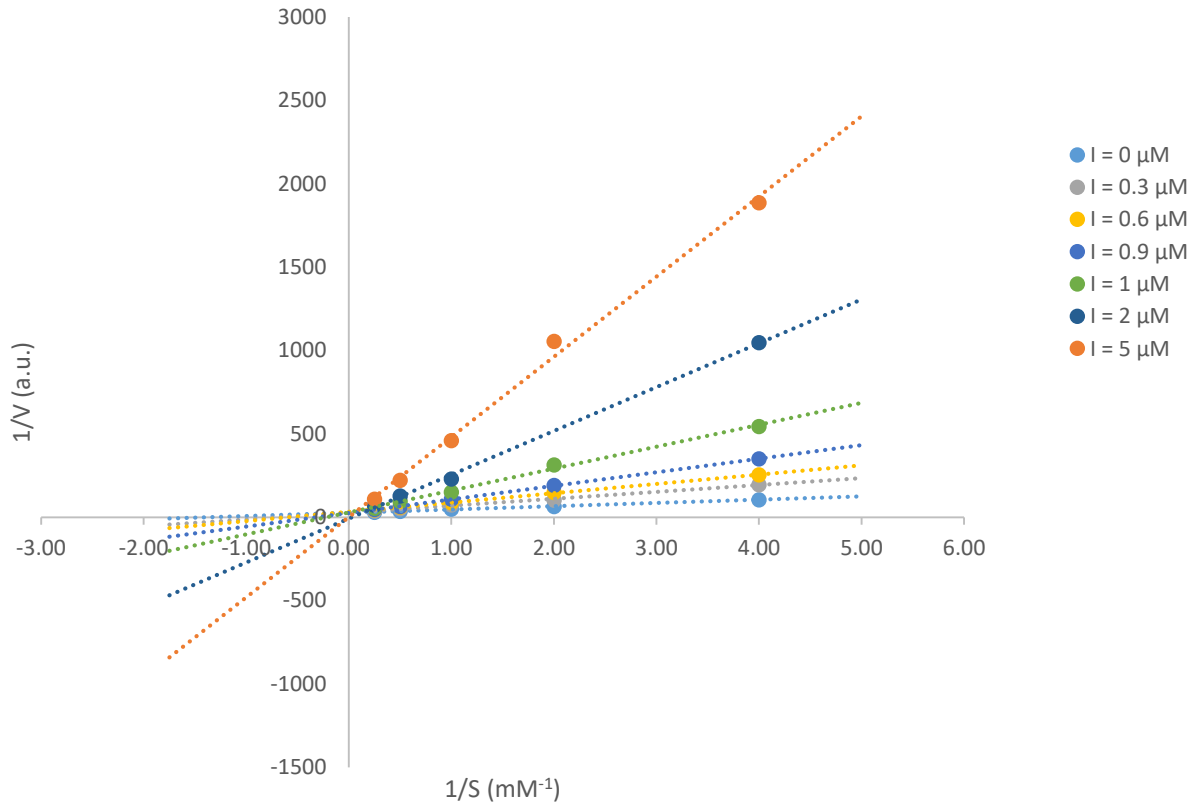


**Figure S37.** Lineweaver-Burk plots and replot of the slope versus inhibitor concentration for  $K_i$  determination of compound AuGNP 5 against JB $\alpha$ -man.

$$K_i = 0.084 \pm 0.066 \mu\text{M}.$$